analytical chemistry

Article

pubs.acs.org/ac

Functional Nucleic Acid Probe for Parallel Monitoring K^+ and Protoporphyrin IX in Living Organisms

Hanjun Cheng,[†,∥] Xuefeng Qiu,[‡] Xiaozhi Zhao,[‡] Wei Meng,[§] Da Huo,[†] and Hui Wei*[,†]

[†]Department of Biomedical Engineering, College of Engineering and Applied Sciences, Collaborative Innovation Center of Chemistry for Life Sciences, Nanjing National Laboratory of Microstructures, Nanjing, Jiangsu 210093, China

[‡]Department of Urology, Nanjing Drum Tower Hospital, The Affiliated Hospital of Nanjing University Medical School, Nanjing, Jiangsu 210008, China

[§]School of Physics, Collaborative Innovation Center of Advanced Microstructures, Nanjing National Laboratory of Microstructures, Nanjing University, Nanjing, Jiangsu 210093, China

[∥]State Key Laboratory of Analytical Chemistry for Life Science, Nanjing University, Nanjing 210093, China

Supporting Information

ABSTRACT: Parallel monitoring of K^+ and protoporphyrin IX (PPIX) is of vital importance because they are not only involved in a variety of biological processes but also closely linked to each other in numerous cellular pathways. However, there are currently no existing methods that can meet the requirements for parallel and in vivo detection of K^+ and PPIX in living organisms. Herein, we demonstrated a functional nucleic acid (FNA)-based technique for parallel monitoring of K^+ and PPIX in living animals. Specifically, the selected G-rich FNA probe was selectively induced to form a parallel G-quadruplex by K^+. The parallel G-quadruplex then remarkably enhanced the fluorescence of PPIX. Thus, by modulating the fluorescence "turn on" with the G-quadruplex and K^+/PPIX, both K^+ and PPIX could be detected. After validating the developed method for selective and sensitive detection of K^+ and PPIX in vitro, their dynamic changes in living organisms (i.e., living brains and tumors) following various physiological and pathological processes were simultaneously monitored. The current study not only provides a general method for the detection of metal ions and bioactive molecules but also presents a way to investigate their synergistic functions in the regulation of various biological processes. It may also be helpful for improving the imaging and therapeutic efficacy of PPIX and 5-ALA.

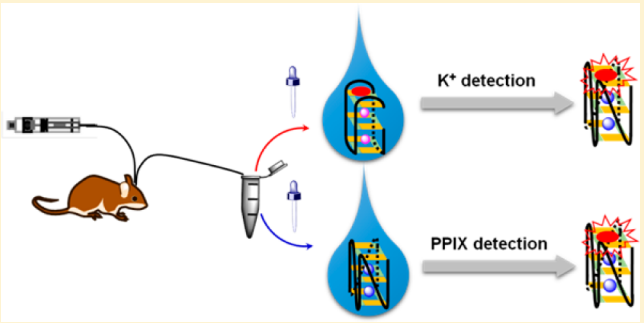

Monitoring metal ions and bioactive small molecules is of particular importance because of their ubiquitous presence in living organisms for a variety of physiological functions.[1−12] For example, potassium ion (K^+) serves particularly important roles in triggering the activation of many signal transduction pathways, maintaining muscular strength, preventing cerebellar granule neuron apoptosis, and so forth.[13−15] The imbalance of K^+ may result in various diseases like vascular diseases and neural dysfunction.[16,17] As an example of bioactive small molecules, protoporphyrin IX (PPIX) is the biosynthesis precursor of heme, which is critical in oxygen transportation-associated energy metabolism and various inflammatory lesions.[18,19] More interestingly, recent studies have revealed that K^+ and PPIX can be closely linked to each other via heme in several ways (Figure S1).[20−22] For example, cellular-free heme derived from PPIX is able to bind to the "ball-and-chain" N terminus of A-type K^+ channels, and the binding enhances the efflux of K^+ and subsequently reduces cellular excitability.[20] Heme could also protect the central nervous systems from reactive oxygen species-induced oxidative stress.[21] These studies imply that both K^+ and PPIX are critical for neural functions and malfunctions (such as cerebral stroke). Furthermore, the two species are also involved in cancer biology.[23−26] For example, the K^+ channel can regulate the blood-brain tumor barrier by increasing its permeability,[24] whereas PPIX serves as a brain tumor biomarker for surgery and photodynamic therapy because of the abnormal heme metabolism-induced PPIX accumulation in cancer cells.[25−27] Therefore, methods for parallel detection of both species in living organisms are greatly needed to gain further understanding of their roles in various physiological and pathological processes, which will be helpful for diagnosis and therapy of related diseases.

To date, many methods have been developed for the individual detection of either K^+ or PPIX alone.[25,27−30] However, the parallel detection of both species remains a great challenge because the current methods for K^+ detection

Received: December 31, 2015
Accepted: January 29, 2016
Published: February 11, 2016

DOI: 10.1021/acs.analchem.5b04936
Anal. Chem. 2016, 88, 2937−2943

are usually not suitable for PPIX detection and vice versa. For example, the orthogonal ion-selective electrodes for K^+ detection does not work for PPIX because the latter is not electrochemically active.[31] Though dual-responsive fluorescent probes to K^+ and PPIX could be developed by ingenious synthesis, they may still not meet the parallel detection requirements due to the potential cross-talk between the two species as well as the wide dynamic range differences of the both species in living organisms (mM range for K^+ and nM to μM range for PPIX). Therefore, effective and facile techniques for parallel detection of both species in living systems are still in great demand. To meet such demands, we herein developed a facile yet effective strategy for parallel monitoring of K^+ and PPIX and their dynamic changes in living organisms (i.e., living brains and tumors) using a G-quadruplex-based functional nucleic acid (FNA) technique (Figure 1 and Figure S2).

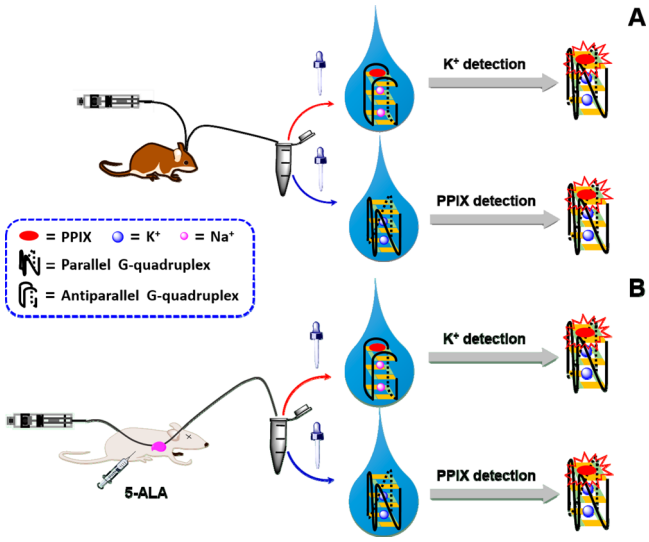

Figure 1. Schematic illustrating the parallel detection of K^+ and PPIX in the brains of living rats (A) and in tumors of living mice (B) using G-quadruplex-based probes.

FNAs are emerging oligonucleotides with intriguing structures and specific biorecognition capabilities.[11,12,32−49] Among the variety of FNAs developed, guanine-rich DNA quadruplexes (G-quadruplexes) have received particular attention in constructing various analytical platforms for biomedical analysis owning to their structural diversity and facile portability.[50−65] For example, Dong and co-workers have recently developed an elegant fluorescent method for selective and sensitive detection of K^+ in lake water by exploring the specific binding of PPIX to parallel G-quadruplex over antiparallel G-quadruplex and duplex DNA.[53] Despite substantial progress, monitoring dynamic changes of biomedically important targets in living organisms with G-quadruplexes remains largely unexplored due to their dramatically different characteristics and large dynamic range variations in living organisms.[66−68]

The peculiar secondary structures of G-quadruplexes are assembled from four-stranded G-rich oligonucleotides through Hoogsteen hydrogen bonds. The assembled G-tetrads are further stabilized by metal ion coordination (typically Na^+ or K^+). More, numerous ligands can bind to G-quadruplexes by stacking onto the G-tetrads, which endows the ligands with enhanced properties, such as enhanced fluorescence for PPIX and improved peroxidase-mimicking activity for hemin.[51,53,54,56,66] By exploring these unique characteristics of G-quadruplexes, we reported here the parallel monitoring metal ion (i.e., K^+) and bioactive small molecule (i.e., PPIX) in living animals with a selected G-quadruplex probe. It has been shown that the selected 18-mer G-rich DNA (referred to as Probe G) was able to form an antiparallel G-quadruplex structure in the presence of Na^+, which was readily transformed into a parallel structure with the addition of K^+.[53] The formed parallel G-quadruplex had a higher affinity toward PPIX, leading to a remarkable enhancement of PPIX fluorescence (Figure S2).[53] In light of this unique K^+-specific fluorescence enhancement of PPIX by the G-quadruplex, fluorescent detection of K^+ and PPIX was established. The K^+ detection was carried out by turning on the fluorescence of the detection solution containing Probe G, PPIX, and Na^+ (referred to as Solution 1) with K^+, and the PPIX detection was accomplished by enhancing its intrinsic fluorescence with the detection solution containing Probe G and K^+ (referred to as Solution 2). After establishing the in vitro detection of K^+ and PPIX with good linearity and excellent selectivity, the parallel monitoring of the dynamic changes of K^+ and PPIX in living organisms (e.g., living brains and tumors) following various physiological and pathological processes was further demonstrated.

EXPERIMENTAL SECTION

Chemicals and Materials. The purified G-rich oligonucleotide 5′-GTGGGTAGGGCGGGTTGG-3′ (Probe G) was obtained from GenScript Biotechnology Co. Ltd. (Nanjing, China).[53] Protoporphyrin IX (PPIX) (Sigma-Aldrich), ascorbic acid (AA) (J&K Scientific), uric acid (UA) (J&K Scientific), dopamine (DA) (Adamas), 3,4-dihydroxyphenylacetic acid (DOPAC) (Accela), 5-hydroxytryptamine (5-HT) (Alfa-Aesar), and 5-aminolevulinic acid (5-ALA) (Aladdin) were used as received. K^+-free artificial cerebrospinal fluid (aCSF) was used as the perfusion solution for in vivo brain microdialysis. The K^+-free aCSF solution was prepared by mixing NaCl (126 mM), $MgCl_2$ (0.85 mM), $NaHCO_3$ (27.5 mM), Na_2SO_4 (0.5 mM), and $CaCl_2$ (1.1 mM) into deionized water, and the solution pH was adjusted to 7.4. K^+-free Ringer's solution was used as the perfusion solution for in vivo tumor microdialysis. The Ringer's solution was prepared by mixing NaCl (147 mM) and $CaCl_2$ (4.4 mM) into deionized water. All aqueous solutions were prepared with deionized water (18.2 MΩ cm, Millipore).

The stock solution of Probe G was prepared in TE buffer (50 mM Tris-HCl, 2.5 mM EDTA, pH 7.0) and quantified using UV−visible absorption spectroscopy with the following extinction coefficients (ε_{260} nm, M^{-1} cm^{-1}) for each nucleotide: A = 15400, G = 11500, C = 7400, and T = 8700. The Probe G solutions were diluted to required concentrations with TE buffer. The resulting Probe G solutions were annealed by heating at 90 °C for 10 min and gradually cooled to room temperature.

Instrumentation. UV−visible absorption spectra were collected on a UV−visible spectrophotometer (Beijing Purkinje General Instrument Co. Ltd., China), and fluorescent spectra were obtained on a Hitachi F-4600 fluorescent spectrometer (Japan). Circular dichroism (CD) spectroscopy of Probe G (20 μM) in the presence of different concentrations of K^+ was measured on a JASCO J-815 CD spectropolarimeter (Tokyo, Japan). Three scans (100 nm min^{-1}) from 210 to 350 at 0.1 nm intervals were accumulated and averaged. The background of

DOI: 10.1021/acs.analchem.5b04936
Anal. Chem. 2016, 88, 2937−2943

the TE buffer solution was subtracted from the original CD data.

The content of PPIX and its analogues in microdialysates was monitored using an Agilent HPLC system consisting of a 1200 quaternary pump solvent delivery system, a degasser, and an autosampler. The column oven temperature was set to 30 °C. Separation was performed on an Agilent Eclipse XDB-C18 column (4.6 × 150 mm, 5 μm) with a mobile phase flow rate of 1 mL/min. The mobile phase was composed of 10% potassium phosphate buffer (10 mM, pH 4.6) and 90% methanol. The wavelength of the fluorescence detector was set to 410 nm for excitation and 620 nm for emission.

Fluorescent Detection of K^+ and PPIX with Probe G. Fluorescent detection of K^+ and PPIX with Probe G was carried out as follows.

For K^+ detection, NaCl and freshly prepared PPIX with appropriate concentrations were added to the diluted Probe G solution to obtain Solution 1, which contained 20 μM Probe G, 20 μM PPIX, and 200 mM Na^+. Solution 1 was incubated at 37 °C in the dark for at least 2 h to achieve structural changes and PPIX binding. Then, Solution 1 was mixed with KCl solutions (or K^+-containing samples) (volume ratio of 1:1). The resultant mixtures were incubated at 37 °C in the dark for at least 2 h and subsequently subjected to fluorescent spectrometric measurements.

For PPIX detection, KCl with an appropriate concentration was added to the diluted Probe G solution to obtain Solution 2, which contained 20 μM Probe G, and 200 mM K^+. Solution 2 was incubated at 37 °C to form K^+-specific G-rich parallel quadruplex structures. The as-prepared Solution 2 was mixed with PPIX solutions (or PPIX-containing samples) (volume ratio of 1:1). After incubating at 37 °C in the dark for PPIX binding, the mixtures were subjected to fluorescent spectrometric measurements.

Parallel Monitoring K^+ and PPIX in Living Rat Brains. The animal studies were approved by the Committee for Experimental Animals Welfare and Ethics of Nanjing Drum Tower Hospital, the Affiliated Hospital of Nanjing University Medical School. Adult male Sprague−Dawley rats (250−300 g) were purchased from Jiesijie Laboratory Animal Co. (Shanghai, China). Rat surgeries were performed as follows.[6] Briefly, the rats were anesthetized with chloral hydrate (345 mg/kg, i.p.) and positioned onto a stereotaxic frame. The microdialysis guide cannulas (MD-2250, Bioanalytical Systems, Inc.) were implanted in the hippocampus of rat (AP = 4.8 mm, L = 5.1 mm from bregma, V = 3.0 mm from dura) using a standard stereotaxic instrument. A stainless steel dummy blocker was then inserted into the implanted guide cannula and fixed until the insertion of a microdialysis probe. After 24 h recovery, a microdialysis probe with a diameter of 0.24 mm (Bioanalytical Systems, Inc.) was implanted into the rat striatum. K^+-free aCSF solution was then continuously perfused at 1 μL min^{-1} for equilibration.

After the equilibration and completed measureming of the basal level for cerebral K^+ and PPIX, a global cerebral ischemia/reperfusion surgery was performed as follows. Through a midline cervical incision, both carotid arteries were exposed and isolated. The global ischemia was induced by occluding both carotid arteries with nontraumatic arterial clips, and reperfusion was realized by subsequently removing the clips. Throughout the surgery, the body temperature of the animals was maintained at 37 °C using a heating pad.

For the parallel detection, the collected brain microdialysate was divided into two halves. One half was 1:1 mixed with Solution 1 for K^+ detection, and the other half was 1:1 mixed with Solution 2 for PPIX detection.

Parallel Monitoring K^+ and PPIX in Tumors in Living Mice. To demonstrate the broad applications of our developed strategy in parallel monitoring K^+ and PPIX in other pathological processes, we selected mice bearing human colonic malignancy xenografts as a tumor model. For generating colon tumors, 12-week-old male Balb/c mice were subcutaneously injected in the right flank with 2 × 10^7 CT-26 cells suspended in 200 μL of buffer. Microdialysis experiments were performed on day 20 after implantation. Tumors of fairly uniform size (approximatelyl 200 to 250 mm^3) were employed. A needle (0.4 × 40 mm) was carefully inserted intracutaneously into the tumor. A linear microdialysis probe (CMA 30) was then guided through the needle. Finally, the needle was removed, leaving the linear microdialysis probe in the tumor. The depth from the epidermis surface to the microdialysis probe was ∼1−2 mm. The linear microdialysis probe was perfused with K^+-free Ringer's solution at 1 μL min^{-1}. The perfusion was run for at least 60 min to achieve equilibration before microdialysis sample collection. The administration of mice with 5-ALA was performed by intraperitoneal injection of the hydrochloric salt of 5-ALA (100 mg/kg, i.p.)

For comparison, microdialysis was also performed at the same position of healthy mice under conditions otherwise identical to those used for tumor-xenografted mice.

RESULTS AND DISCUSSION

In Vitro Detection of K^+ and PPIX Using G-quadruplex. First, the feasibility of the proposed strategy for in vitro detection of K^+ and PPIX was investigated. The K^+ detection was carried out by inducing the antiparallel-to-parallel conformational transition of the G-quadruplex with K^+ and thus turning on the fluorescence of Probe G-PPIX complex (Figure 2A, inset). The addition of K^+ into Solution 1 led to a significant fluorescence enhancement of complexed PPIX, and the fluorescent intensity increased with the increase of K^+ concentration (Figure 2A). As shown in Figure 2B, the ratio of enhanced PPIX fluorescence to the unenhanced one (i.e., $(F_1 - F_0)/F_0$) exhibited a good linearity toward K^+ concentration

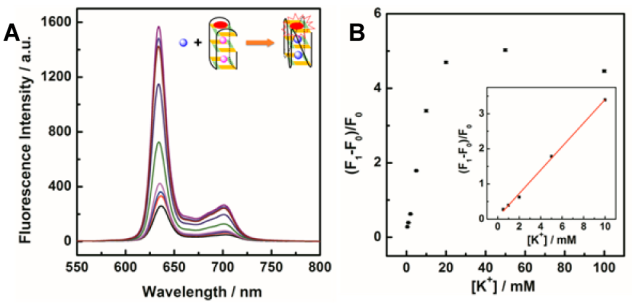

Figure 2. (A) Typical fluorescence responses of 10 μM Probe G-PPIX complex in the presence of 100 mM Na^+ to different concentrations of K^+. λ_{ex} = 410 nm. Inset: schematic illustrating the K^+ detection with the as-formed antiparallel Probe G-PPIX complex. (B) Dependence of fluorescence changes of Probe G-PPIX complex on K^+ concentrations. F_0 and F_1 represent the fluorescence intensity at 635 nm of Probe G-PPIX complex in the absence and presence of K^+, respectively. Inset: plot of $(F_1 - F_0)/F_0$ versus K^+ concentration. Error bars indicate standard deviations of three independent measurements.

DOI: 10.1021/acs.analchem.5b04936
Anal. Chem. 2016, 88, 2937−2943

ranging from 500 μM to 10 mM ($(F_1 - F_0)/F_0 = 0.335 \times [K^+]$ mM^{-1} + 0.056, R^2 = 0.997), which covers the physiological concentrations of K^+ in living organisms. A detection limit of 100 μM was obtained with the current FNA biotechnology.

The PPIX detection was accomplished by enhancing its intrinsic fluorescence upon binding to the parallel G-quadruplex-PPIX complex (Figure 3A, inset). As depicted in

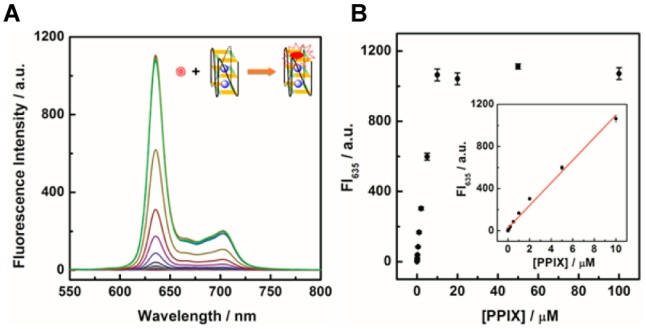

Figure 3. (A) Typical fluorescence responses of 10 μM Probe G-PPIX complex in the presence of 100 mM K^+ to different concentrations of PPIX. λ_{ex} = 410 nm. Inset: schematic illustrating the PPIX detection with the as-formed parallel G-quadruplex complex. (B) Dependence of fluorescence changes of Probe G-PPIX complex on PPIX concentrations. FI_{635} represents the fluorescence intensity at 635 nm. Inset: plot of FI_{635} versus PPIX concentration. Error bars indicate standard deviations of three independent measurements.

Figure 3, the fluorescence of PPIX increased with the increase of PPIX concentration. Moreover, the fluorescence intensity showed a linear response toward PPIX concentration ranging from 10 nM to 10 μM (FI_{635} = 107.27 × [PPIX] μM^{-1} + 25.48), which covers the physiological concentrations of PPIX in living organisms. The detection limit was as low as 0.5 nM, which was much better than that using PPIX intrinsic fluorescence alone (Figure S4).

Highly Selective Detection of K^+ and PPIX without Cross Talk. It is critical to evaluate the selectivity of the current method for detection of K^+ and PPIX because of the chemical and physiological complexity of living organisms. For this purpose, the potential interference from commonly coexisting bioactive small molecules was investigated first. As shown in Figure S5, the presence of several biochemicals (such as glucose, lactate, AA, 5-HT, UA, DA, and DOPAC) at their physiological concentrations did not result in an obvious change in the fluorescence signals. Furthermore, the selectivity against biologically important metal ions in living systems was examined. As shown in Figure S5, the presence of the metal ions produced almost identical fluorescence responses when compared with the pristine testing solution, suggesting that these metal ions had no interference toward K^+ and PPIX detection. Such good selectivity was mainly ascribed to the high affinity of Probe G toward K^+ and PPIX as well as the masking effects of the added EDTA toward those metal ions. The Na^+-independent response essentially allows the Probe G-based detection technique for parallel monitoring K^+ and PPIX during complicated pathological processes (e.g., ischemic stroke) in which the concentration of Na^+ undergoes dramatic changes (Figure S6).

To homogeneously detect the coexisting K^+ and PPIX in living organisms without sample separation, it is also essential to evaluate the potential cross-talk between K^+ and PPIX detection. This is because the fluorescence detection signals depend on both K^+ and PPIX and fluctuation of either of their concentrations may affect the fluorescence response of the other. To this end, the saturated concentration of one species was used for the detection of the other (i.e., for K^+ detection, 10 μM of PPIX was added in Solution 1, and for PPIX detection, 100 mM of K^+ was added in Solution 2). Thus, the final concentration increase of one species would not affect the detection of the other. As shown in Figure S7A, for K^+ detection, the further addition of 200 nM PPIX into Solution 1 containing 2 mM of K^+ led to negligible fluorescence changes. Similarly, for PPIX detection, the further addition of 5 mM K^+ into Solution 2 containing 1 μM of PPIX did not result in an obvious fluorescence change either (Figure S7B). These results substantially demonstrated that no cross talk occurred in parallel measurements of K^+ and PPIX with the current method.

The excellent analytical performance (i.e., high selectivity, remarkable sensitivity, and physiologically related dynamic ranges) enables the FNA-based detection technique to simultaneously monitor the dynamic changes of K^+ and PPIX in living organisms, as will be discussed below.

Parallel and In Vivo Detection of K^+ and PPIX in Living Brains. The parallel detection of K^+ and PPIX in living organisms with the current method was first validated in living brains of rats (Figure 1A). As shown in Figure 4A, for in vivo

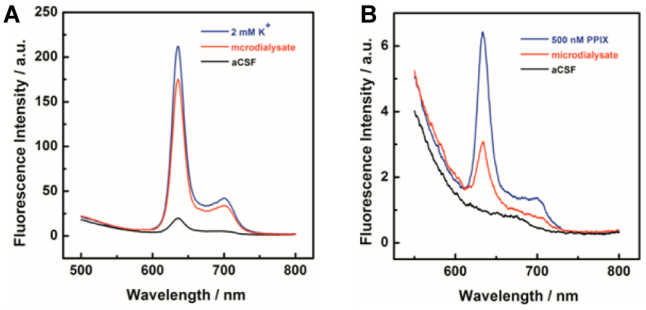

Figure 4. Typical fluorescence responses to K^+ (A) or PPIX (B) in living brain microdialysates. λ_{ex} = 410 nm.

K^+ detection, the addition of the brain microdialysate into Solution 1 resulted in a remarkable enhancement of PPIX fluorescence compared with the intrinsic fluorescence of K^+-free aCSF mixed with Solution 1, suggesting the presence of K^+ in the living brain microdialysate. To further confirm the accuracy and reliability of the current method, an orthogonal method (i.e., inductive coupled plasma atomic absorption spectrophotometry (ICP-AAS)) was also employed to measure the K^+ concentrations in the brain microdialysates. As summarized in Table S1, the K^+ concentrations in the brain microdialysates measured by our method matched well with the ones by ICP-AAS, validating the effective measurements of K^+ in living brains with the current method. Meanwhile, for PPIX detection, the addition of the brain microdialysate into Solution 2 led to a prominent fluorescence, suggesting the existence of PPIX in brain microdialysates (Figure 4B). Compared with the extremely weak fluorescence of pristine brain microdialysate, the uses of the K^+-specific parallel G-quadruplex significantly improved the fluorescence response for in vivo PPIX detection (Figure S8).

After establishing the in vivo measurements of K^+ and PPIX in the living brain of rats with our method, parallel monitoring of the dynamic changes of K^+ and PPIX in the hippocampus of

DOI: 10.1021/acs.analchem.5b04936
Anal. Chem. 2016, 88, 2937−2943

living rats following ischemia/reperfusion was carried out.[8] As shown in Figure 5, the basal levels of K^+ and PPIX were

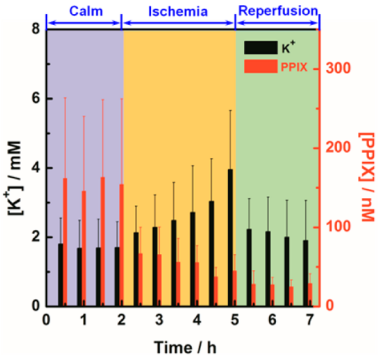

Figure 5. Dynamic changes of K^+ and PPIX in the hippocampus of living rats following ischemia/reperfusion. Data are presented as mean ± SD.

determined to be 1.81 ± 0.75 mM and 161.8 ± 101.7 nM (n = 4), respectively. When the rats were administered global ischemia for 3 h, the extracellular K^+ concentration gradually increased to 3.96 ± 1.70 mM (n = 4). Surprisingly, the level of PPIX dramatically decreased to 67.0 ± 33.2 nM (n = 4) after 1 h of global ischemia and then gradually decreased to 45.0 ± 20.5 nM (n = 4). After 2 h of reperfusion, the level of K^+ was gradually decreased to 1.91 ± 1.15 mM (n = 4), which was nearly restored to its basal level. The PPIX level, however, underwent a continuous decrease to 29.0 ± 12.3 nM (n = 4). Although the exact neurochemical mechanism for the observed mirroring behaviors of K^+ and PPIX following ischemia is still unclear, we made the following assumption: when the rats were subjected to cerebral ischemia, the K^+ channels of neurons were depolarized and large numbers of hemoglobin-containing red blood cells were released, leading to a subsequent release of heme from hemoglobin.[69] Several pathways were subsequently activated to transport and metabolize the released heme and its iron moiety, which would protect the brain from potential oxidative stress.[69] The released heme could also bind to A-type K^+ channels, allowing for a greater efflux of K^+.[20] Meanwhile, the extracellular PPIX was taken up by neurons to reproduce exhausted heme. During the reperfusion process, the elevated K^+ was taken up again and redistributed to prevent the ion imbalance because of the K^+ homeostasis capability of astrocytes. Because PPIX is the precursor of heme biosynthesis and cannot be directly supplied from blood flow, it may need a longer time to be restored to its basal levels. Although more studies are needed to further elucidate the possible mechanism for the observed dynamic changes of K^+ and PPIX, the current results substantially suggest that the developed FNA technique can be used for effectively probing the synergetic roles of metal ions and small molecules involved in living brains.

Parallel and In Vivo Detection of K^+ and PPIX in Living Tumors. The practical application of our developed FNA technique was further validated in parallel and in vivo measurements of K^+ and PPIX in tumors because both also play important roles in tumor metabolism, proliferation, and necrosis. As shown in Figure 6, the basal level of K^+ in the colon tumor group was determined to be 2.05 ± 0.54 mM (n = 3), which was ~2-fold higher than that for the healthy group (0.95 ± 0.09 mM (n = 3)). Such a difference might be ascribed to the necrosis of tumor cells and the subsequent release of K^+

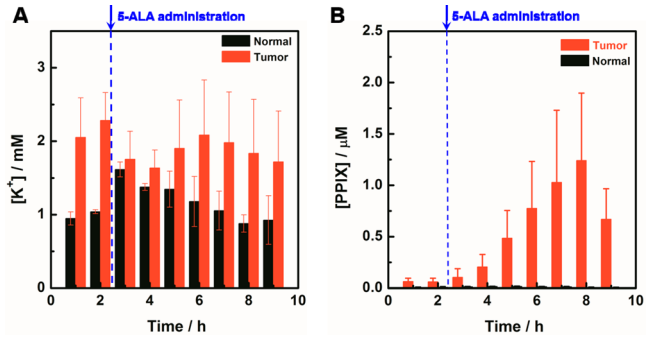

Figure 6. Dynamic changes of K^+ (A) and PPIX (B) in tumor-bearing (red bars) or healthy (black bars) mice before and after the administration of 5-ALA. Data are presented as mean ± SD.

into intercellular fluid.[23] The basal levels of PPIX for the tumor-bearing mice, however, was nearly 10-fold higher than that of healthy mice (64.1 ± 31.1 vs 6.6 ± 3.3 nM, n = 3).

After the administration of mice with 5-ALA, the precursor of PPIX, the PPIX levels in the tumor group dramatically increased to 1.24 ± 0.66 μM (n = 3) while no prominent changes of K^+ levels were observed in the same group (Figure 6). For the healthy group, however, the K^+ level sharply increased after the administration of 5-ALA and then gradually decreased to its basal level. The PPIX level in the healthy group underwent much smaller changes after 5-ALA administration when compared with that for the tumor group (Figure 6B and Figure S12). According to early studies, exogenous 5-ALA was first transformed to PPIX by a series of 5-ALA synthases, which was subsequently incorporated with iron ions to biosynthesize heme with the help of ferrochelatase.[18,70] The increased K^+ level in the healthy group after 5-ALA administration might be ascribed to the efflux of K^+ upon the binding of the produced heme to K^+ channels, as mentioned above (Figure S1). On the other hand, because of the higher activity of porphobilinogen deaminase (the enzyme for transforming 5-ALA into PPIX) and the lower activity of ferrochelatase in tumors, the biosynthesis of heme from PPIX was blocked.[18,70] Such blockage would result in significant accumulation of PPIX in tumors, as evidenced by the much higher concentration of PPIX in the tumor group as compared to that of the healthy group. Because 5-ALA is clinically used in tumor imaging and therapy, these results essentially demonstrated that the developed FNA technique offered an effective platform for investigation of the pharmacokinetics of 5-ALA as well as for evaluation of the imaging performance and therapeutic efficacy of 5-ALA. Note also that the current method is applicable to other tumors. For instance, PPIX content in glioma-bearing mice before and after the administration of 5-ALA could also be monitored (Figure S13).

CONCLUSIONS

In summary, we demonstrated a facile yet effective method to simultaneously quantify K^+ and PPIX in living organisms by exploring the K^+-induced antiparallel-to-parallel conformational transition of the G-quadruplex and the parallel G-quadruplex-enhanced fluorescence of PPIX. The FNA technique-based method showed numerous merits, such as high sensitivity, remarkable selectivity, robust reliability, and wide dynamic range. After evaluating the method for the detection of K^+ and PPIX in vitro, it was successfully used to simultaneously monitor the dynamic changes of K^+ and PPIX in brains and

DOI: 10.1021/acs.analchem.5b04936
Anal. Chem. 2016, 88, 2937−2943

tumors of living animals following various physiological and pathological processes. The current work not only offers a new strategy to monitor physiologically important species in living systems but also provides an effective platform to better understand the synergistic roles of K^+ and PPIX in regulating various biological processes. Moreover, the developed method is applicable to other systems (such as Cu^{2+} and heme for Alzheimer's disease).[71]

■ ASSOCIATED CONTENT

Supporting Information

The Supporting Information is available free of charge on the ACS Publications website at DOI: 10.1021/acs.analchem.5b04936.

K^+ concentration measurements, scheme of the potential linkage among the cellular pathways involving K^+ and PPIX, schematic illustration of K^+-induced antiparallel-to-parallel conformational transition of the G-quadruplex and the remarkable fluorescence enhancement of PPIX by the parallel G-quadruplex for K^+ and PPIX detection, CD spectra, typical fluorescence responses, evaluation of potential cross talk between K^+ and PPIX, HPLC chromatograms, and dynamic changes and content of PPIX following 5-ALA administration (PDF)

■ AUTHOR INFORMATION

Corresponding Author

*E-mail: weihui@nju.edu.cn. Fax: +86-25-83594648. Tel: +86-25-83593272.

Notes

The authors declare the following competing financial interest: H.W. and J.C. are co-authors on patent applications.

■ ACKNOWLEDGMENTS

This work was supported by National Natural Science Foundation of China (21405079, 21405081), Natural Science Foundation of Jiangsu Province (BK20130561), 973 Program (2015CB659400), PAPD program, Fundamental Research Funds for Central Universities (no. 20620140617, 20620140627), Shuangchuang Program of Jiangsu Province, Six Talents Summit Program of Jiangsu Province, Open Funds of the State Key Laboratory of Electroanalytical Chemistry (SKLEAC201501), Open Funds of the State Key Laboratory of Analytical Chemistry for Life Science (SKLACLS1404), and Thousand Talents Program for Young Researchers. We would like to thank Professor Yong Hu for help with animal studies, Professor Yi Cao for use of the CD spectrometer, and Ms Min Zhou and Professors Andrew Ellington and Itamar Willner for insightful discussions and comments.

■ REFERENCES

(1) Luo, Y.; Zhang, L.; Liu, W.; Yu, Y.; Tian, Y. *Angew. Chem., Int. Ed.* **2015**, *54*, 14053−14056.
(2) Carter, K. P.; Young, A. M.; Palmer, A. E. *Chem. Rev.* **2014**, *114*, 4564−4601.
(3) Murray, I. A.; Patterson, A. D.; Perdew, G. H. *Nat. Rev. Cancer* **2014**, *14*, 801−814.
(4) Huang, P. C.; Wu, F. Y.; Mao, L. Q. *Anal. Chem.* **2015**, *87*, 6834−6841.
(5) Li, X. C.; Zhao, L. Z.; Chen, Z. L.; Lin, Y. Q.; Yu, P.; Mao, L. Q. *Anal. Chem.* **2012**, *84*, 5285−5291.
(6) Lin, Y.; Yu, P.; Hao, J.; Wang, Y.; Ohsaka, T.; Mao, L. *Anal. Chem.* **2014**, *86*, 3895−3901.
(7) Zhang, L. M.; Han, Y. Y.; Zhao, F.; Shi, G. Y.; Tian, Y. *Anal. Chem.* **2015**, *87*, 2931−2936.
(8) Cheng, H. J.; Wang, X. Y.; Wei, H. *Anal. Chem.* **2015**, *87*, 8889−8895.
(9) Zhu, A. W.; Qu, Q.; Shao, X. L.; Kong, B.; Tian, Y. *Angew. Chem., Int. Ed.* **2012**, *51*, 7185−7189.
(10) Chai, X. L.; Zhou, X. G.; Zhu, A. W.; Zhang, L. M.; Qin, Y.; Shi, G. Y.; Tian, Y. *Angew. Chem., Int. Ed.* **2013**, *52*, 8129−8133.
(11) Huang, P. J. J.; Wang, F.; Liu, J. W. *Anal. Chem.* **2015**, *87*, 6890−6895.
(12) Huang, P. J. J.; Vazin, M.; Liu, J. W. *Anal. Chem.* **2015**, *87*, 10443−10449.
(13) Segovia, J.; Sabbah, A.; Mgbemena, V.; Tsai, S. Y.; Chang, T. H.; Berton, M. T.; Morris, I. R.; Allen, I. C.; Ting, J. P. Y.; Bose, S. *PLoS One* **2012**, *7*, 15.
(14) Petkov, G. V. *Nat. Rev. Urol.* **2012**, *9*, 30−40.
(15) Jekabsons, M. B.; Nicholls, D. G. *Cell Death Differ.* **2006**, *13*, 1595−1610.
(16) Sobey, C. G. *Arterioscler., Thromb., Vasc. Biol.* **2001**, *21*, 28−38.
(17) Leis, J. A.; Bekar, L. K.; Walz, W. *Glia* **2005**, *50*, 407−416.
(18) Peng, Q.; Berg, K.; Moan, J.; Kongshaug, M.; Nesland, J. M. *Photochem. Photobiol.* **1997**, *65*, 235−251.
(19) Wachowska, M.; Muchowicz, A.; Firczuk, M.; Gabrysiak, M.; Winiarska, M.; Wanczyk, M.; Bojarczuk, K.; Golab, J. *Molecules* **2011**, *16*, 4140−4164.
(20) Sahoo, N.; Goradia, N.; Ohlenschlager, O.; Schonherr, R.; Friedrich, M.; Plass, W.; Kappl, R.; Hoshi, T.; Heinemann, S. H. *Proc. Natl. Acad. Sci. U. S. A.* **2013**, *110*, E4036−E4044.
(21) Dore, S.; Goto, S.; Sampei, K.; Blackshaw, S.; Hester, L. D.; Ingi, T.; Sawa, A.; Traystman, R. J.; Koehler, R. C.; Snyder, S. H. *Neuroscience* **2000**, *99*, 587−592.
(22) Willis, D.; Moore, A. R.; Frederick, R.; Willoughby, D. A. *Nat. Med.* **1996**, *2*, 87−90.
(23) Nietsch, H. H.; Roe, M. W.; Fiekers, J. F.; Moore, A. L.; Lidofsky, S. D. *J. Biol. Chem.* **2000**, *275*, 20556−20561.
(24) Ningaraj, N. S.; Rao, M.; Hashizume, K.; Asotra, K.; Black, K. L. *J. Pharmacol. Exp. Ther.* **2002**, *301*, 838−851.
(25) Valdes, P. A.; Leblond, F.; Kim, A.; Harris, B. T.; Wilson, B. C.; Fan, X.; Tosteson, T. D.; Hartov, A.; Ji, S.; Erkmen, K.; Simmons, N. E.; Paulsen, K. D.; Roberts, D. W. *J. Neurosurg.* **2011**, *115*, 11−17.
(26) Liao, H.; Noguchi, M.; Maruyama, T.; Muragaki, Y.; Kobayashi, E.; Iseki, H.; Sakuma, I. *Med. Image Anal.* **2012**, *16*, 754−766.
(27) Kairdolf, B. A.; Bouras, A.; Kaluzova, M.; Sharma, A. K.; Wang, M. D.; Hadjipanayis, C. G.; Nie, S. *Anal. Chem.* **2016**, *88*, 858−867.
(28) Kim, B.; Jung, I. H.; Kang, M.; Shim, H.-K.; Woo, H. Y. *J. Am. Chem. Soc.* **2012**, *134*, 3133−3138.
(29) Kong, X.; Su, F.; Zhang, L.; Yaron, J.; Lee, F.; Shi, Z.; Tian, Y.; Meldrum, D. R. *Angew. Chem., Int. Ed.* **2015**, *54*, 12053−12057.
(30) Vahrmeijer, A. L.; Hutteman, M.; van der Vorst, J. R.; van de Velde, C. J. H.; Frangioni, J. V. *Nat. Rev. Clin. Oncol.* **2013**, *10*, 507−518.
(31) Otto, M.; Thomas, J. D. R. *Anal. Chem.* **1985**, *57*, 2647−2651.
(32) Ellington, A. D.; Szostak, J. W. *Nature* **1990**, *346*, 818−822.
(33) Liu, J. W.; Cao, Z. H.; Lu, Y. *Chem. Rev.* **2009**, *109*, 1948−1998.
(34) Famulok, M.; Mayer, G. *Acc. Chem. Res.* **2011**, *44*, 1349−1358.
(35) Du, Y.; Li, B. L.; Wang, E. K. *Acc. Chem. Res.* **2013**, *46*, 203−213.
(36) Liang, H.; Zhang, X. B.; Lv, Y. F.; Gong, L.; Wang, R. W.; Zhu, X. Y.; Yang, R. H.; Tan, W. H. *Acc. Chem. Res.* **2014**, *47*, 1891−1901.
(37) Wang, F.; Liu, X.; Willner, I. *Angew. Chem., Int. Ed.* **2015**, *54*, 1098−1129.
(38) Wei, H.; Li, B. L.; Li, J.; Wang, E. K.; Dong, S. J. *Chem. Commun.* **2007**, 3735−3737.
(39) Wei, H.; Li, B. L.; Li, J.; Dong, S. J.; Wang, E. K. *Nanotechnology* **2008**, *19*, 095501.
(40) Wang, B.; Guo, C. L.; Chen, G. J.; Park, B.; Xu, B. Q. *Chem. Commun.* **2012**, *48*, 1644−1646.
(41) Chen, G.; Liu, D.; He, C.; Gannett, T. R.; Lin, W.; Weizmann, Y. *J. Am. Chem. Soc.* **2015**, *137*, 3844−3851.

DOI: 10.1021/acs.analchem.5b04936
Anal. Chem. 2016, 88, 2937−2943

(42) Ma, D.-L.; Zhang, Z.; Wang, M.; Lu, L.; Zhong, H.-J.; Leung, C.-H. *Chem. Biol.* **2015**, *22*, 812−828.
(43) Shastri, A.; McGregor, L. M.; Liu, Y.; Harris, V.; Nan, H. Q.; Mujica, M.; Vasquez, Y.; Bhattacharya, A.; Ma, Y. T.; Aizenberg, M.; Kuksenok, O.; Balazs, A. C.; Aizenberg, J.; He, X. M. *Nat. Chem.* **2015**, *7*, 447−454.
(44) Xiang, Y.; Lu, Y. *Nat. Chem.* **2011**, *3*, 697−703.
(45) Jia, X. F.; Li, J.; Wang, E. K. *Chem. - Eur. J.* **2012**, *18*, 13494−13500.
(46) Jia, X. F.; Li, J.; Han, L.; Ren, J. T.; Yang, X.; Wang, E. K. *ACS Nano* **2012**, *6*, 3311−3317.
(47) Gu, W. L.; Deng, X.; Gu, X. X.; Jia, X. F.; Lou, B. H.; Zhang, X. W.; Li, J.; Wang, E. K. *Anal. Chem.* **2015**, *87*, 1876−1881.
(48) Wang, B.; Guo, C. L.; Zhang, M. M.; Park, B.; Xu, B. Q. *J. Phys. Chem. B* **2012**, *116*, 5316−5322.
(49) Peri-Naor, R.; Ilani, T.; Motiei, L.; Margulies, D. *J. Am. Chem. Soc.* **2015**, *137*, 9507−9510.
(50) Zhu, J.; Zhang, L.; Dong, S.; Wang, E. *Chem. Sci.* **2015**, *6*, 4822−4827.
(51) Travascio, P.; Li, Y. F.; Sen, D. *Chem. Biol.* **1998**, *5*, 505−517.
(52) Zhang, L. B.; Zhu, J. B.; Guo, S. J.; Li, T.; Li, J.; Wang, E. K. *J. Am. Chem. Soc.* **2013**, *135*, 2403−2406.
(53) Li, T.; Wang, E.; Dong, S. *Anal. Chem.* **2010**, *82*, 7576−7580.
(54) Tan, X. H.; Wang, Y.; Armitage, B. A.; Bruchez, M. P. *Anal. Chem.* **2014**, *86*, 10864−10869.
(55) Liu, Z.; Li, W.; Nie, Z.; Peng, F.; Huang, Y.; Yao, S. *Chem. Commun.* **2014**, *50*, 6875−6878.
(56) Huang, H.; Suslov, N. B.; Li, N.-S.; Shelke, S. A.; Evans, M. E.; Koldobskaya, Y.; Rice, P. A.; Piccirilli, J. A. *Nat. Chem. Biol.* **2014**, *10*, 686−691.
(57) Lin, S.; Gao, W.; Tian, Z. R.; Yang, C.; Lu, L. H.; Mergny, J. L.; Leung, C. H.; Ma, D. L. *Chem. Sci.* **2015**, *6*, 4284−4290.
(58) Leung, K. H.; He, H. Z.; He, B. Y.; Zhong, H. J.; Lin, S.; Wang, Y. T.; Ma, D. L.; Leung, C. H. *Chem. Sci.* **2015**, *6*, 2166−2171.
(59) Ai, J.; Li, T.; Li, B. L.; Xu, Y. H.; Li, D.; Liu, Z. J.; Wang, E. K. *Anal. Chim. Acta* **2012**, *741*, 93−99.
(60) Zhou, Z. X.; Li, D.; Zhang, L. B.; Wang, E. K.; Dong, S. J. *Talanta* **2015**, *134*, 298−304.
(61) Li, T.; Wang, E. K.; Dong, S. J. *J. Am. Chem. Soc.* **2009**, *131*, 15082−15083.
(62) Zhou, Z. X.; Zhu, J. B.; Zhang, L. B.; Du, Y.; Dong, S. J.; Wang, E. K. *Anal. Chem.* **2013**, *85*, 2431−2435.
(63) Ren, J. T.; Wang, T. S.; Wang, E. K.; Wang, J. *Analyst* **2015**, *140*, 2556−2572.
(64) Zhu, J. B.; Zhang, L. B.; Teng, Y.; Lou, B. H.; Jia, X. F.; Gu, X. X.; Wang, E. K. *Nanoscale* **2015**, *7*, 13224−13229.
(65) Margulies, D.; Hamilton, A. D. *Angew. Chem., Int. Ed.* **2009**, *48*, 1771−1774.
(66) Tseng, T. Y.; Wang, Z. F.; Chien, C. H.; Chang, T. C. *Nucleic Acids Res.* **2013**, *41*, 10605−10618.
(67) Li, R. M.; Jiang, Q.; Cheng, H. J.; Zhang, G. Q.; Zhen, M. M.; Chen, D. Q.; Ge, J. C.; Mao, L. Q.; Wang, C. R.; Shu, C. Y. *Analyst* **2014**, *139*, 1993−1999.
(68) Biffi, G.; Tannahill, D.; McCafferty, J.; Balasubramanian, S. *Nat. Chem.* **2013**, *5*, 182−186.
(69) Wagner, K. R.; Sharp, F. R.; Ardizzone, T. D.; Lu, A. G.; Clark, J. F. *J. Cereb. Blood Flow Metab.* **2003**, *23*, 629−652.
(70) Pogue, B. W.; Gibbs-Strauss, S. L.; Valdes, P. A.; Samkoe, K. S.; Roberts, D. W.; Paulsen, K. D. *IEEE J. Sel. Top. Quantum Electron.* **2010**, *16*, 493−505.
(71) Ghosh, C.; Seal, M.; Mukherjee, S.; Dey, S. G. *Acc. Chem. Res.* **2015**, *48*, 2556−2564.

DOI: 10.1021/acs.analchem.5b04936
Anal. Chem. 2016, 88, 2937−2943